캔틸레버 복합 적층판의 3차원 진동해석

Three-Dimensional Vibration Analysis of Cantilevered Laminated Composite Plates

김 주 우* 정 희 영**
Kim, Joo-Woo Jung, Hie-young
(논문접수일 : 2000년 11월 16일 ; 심사종료일 : 2001년 8월 21일)

요 지

본 논문은 캔틸레버 복합 적층판의 고유진동에 대하여 3차원으로 해석한 연구를 제시하고 있다. 본 연구에서는 고정단에서의 경계조건을 엄밀히 만족하고 수학적으로 완전한 다항식으로 표현되는 근사 변위와 Ritz 방법을 이용하여 Lagrangian범함수의 정상값을 구하였다. 3차원 모델의 정확도는 무차원 진동수의 수렴연구를 통하여 이루어졌으며, 또한 기존 문헌상의 해석 및 실험 결과와의 비교를 통하여 본 연구 결과의 정확성을 검토하였다. 본 논문에서 제시된 3차원 진동수의 결과를 이용하여 캔틸레버 복합 적층판의 기하학 및 재료 매개변수 즉, 형상비(a/b), 폭두께비(a/h), 재료의 직교 이방성, 플라이 수(NP), 섬유 배향각(θ), 및 적층 순서가 미치는 효과를 설명하였다.

핵심용어 : Ritz 방법, 3차원 모델, 고유진동, 복합 적층판, 재료의 직교이방성

Abstract

This paper presents the three-dimensional (3-D) study of the natural vibration of cantilevered laminated composite plates. The Ritz method is used to obtain stationary values of the associated Lagrangian functional with displacements approximated by mathematically complete polynomials satisfying the boundary conditions at the clamped edge exactly. The accuracy of the 3-D model is established through a convergence study of non-dimensional frequencies followed by a comparison of the converged 3-D solutions with analytical and experimental findings in the existing literature. A wide scope of 3-D frequency results explain the influence of a number of geometrical and material parameters for cantilevered laminated plates, namely aspect ratio (a/b), width-to-thickness ratio (a/h), orthotropy of material, number of plies (NP), fiber orientation angle (θ), and stacking sequence.

Keywords : *Ritz method, three-dimensional model, natural vibration, laminated composite plate, orthotropy of material*

1. Introduction

Documented in the published literature over two decades are some fundamental investigations, which specifically address, both theoretically and experimentally, the vibration problem of a cantilevered laminated composite plate.[1)~5)] Much of the previous work done on the subject[6)] employed classical lamination theory (CLT) which assumes a mathematical model comprising of a

* 정회원 · 세명대학교 건축공학과, 조교수
** 정회원 · 서울시립대학교 토목공학과, 부교수

• 이 논문에 대한 토론을 2001년 12월 31일까지 본 학회에 보내주시면 2002년 3월호에 그 결과를 게재하겠습니다.

number of orthotropic thin-plate layers perfectly bonded with non-shear-deformable infinitely thin bondlines. In constructing the kinematics of each lamina, investigators assumed Kirchhoff's postulates of normals to the mid-plane before deformation remain so after deformation. With such models, higher upper bounds on the true natural frequencies are produced, somewhat marginally in the lower modes; however, quite significantly in the higher modes. These inaccurate frequency solutions are primarily attributed to the absence of transverse shear strains in the classical approach, which may be considerable in thin, as well as thick, fibrous composite plates.

Modern advanced composite materials have a high elastic-to-transverse shear modulus ratio. Moreover, such materials may be employed in structural applications calling for plates having a low width-to-thickness ratio in order to maximize the overall strength-to-weight ratio. Consequentially, the inclusion of transverse shear deformation in the kinematics of laminated composite plates is essential to the accuracy of the mathematical model.

Consider the cantilevered laminated composite plate shown in Fig. 1. The dimensions of plate are length a, width b and thickness h. This study offers a 3-D elasticity-based kinematics and constitutive model of each laminae, resulting in a higher-order *smear* approximation of the transverse shear strains across the thickness of the plate laminate. In this analysis, the dynamical energies are formulated for a plate lamination comprising of N orthotropic parallelepiped layers with thickness t_p, fiber orientation angle θ, and perfectly bonded with non-shear-deformable infinitely thin bondlines. The in-plane (u, v) and transverse (w) displacements are directed along the x, y, z coordinate directions, respectively. These displacements are assumed as simple polynomials, which are mathematically complete and which satisfy the vanishing displacements at the clamped end exactly. The Ritz method is used to extremize the associated Lagrangian so as to obtain upper bound approximate natural frequencies close to the exact ones, as sufficient numbers of polynomial terms are retained.

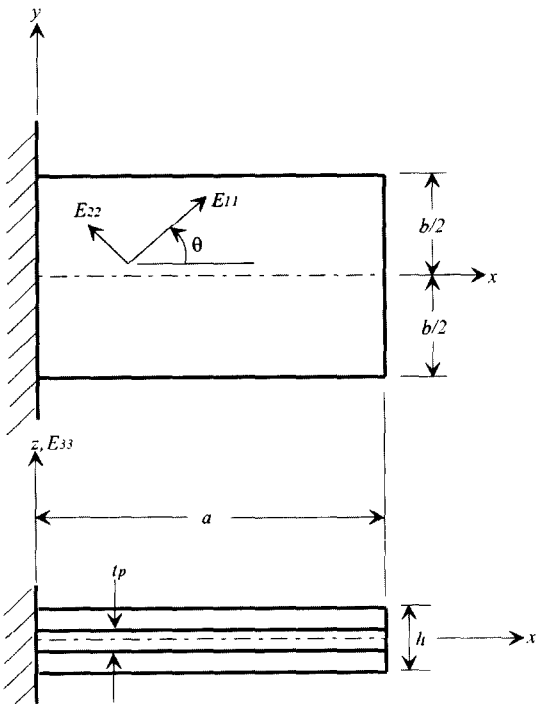

Fig. 1 Cantilevered laminated composite plate

The accuracy of the present three-dimensional method is established through comparisons of frequency data with analytical and experimental findings in the published literature. Non-dimensional frequencies are presented for the effect of several parameters connected to symmetrically laminated composite plate vibrations, namely aspect ratio (a/b), thickness ratio (a/h), orthotropy of material, number of plies (NP), fiber orientation angle (θ), and stacking sequence.

2.Theoretical Formulation

The strain vector $\{\varepsilon\}$ is related to the dis-

placements u, v, and w along the Cartesian coordinates (x, y, z) of the plate(or parallelepiped) shown in Fig. 1,

$$\{\varepsilon\}=\{\varepsilon_x, \varepsilon_y, \varepsilon_z, \gamma_{xy}, \gamma_{yz}, \gamma_{xz}\}^T \tag{1}$$

where $\{\varepsilon\}$ is the linear classical strain vector containing the following displacement gradients:

$$\varepsilon_x=\frac{\partial u}{\partial x};\ \varepsilon_y=\frac{\partial u}{\partial y};\ \varepsilon_z=\frac{\partial w}{\partial z};$$
$$\gamma_{xy}=\frac{\partial u}{\partial y}+\frac{\partial v}{\partial x};\ \gamma_{yz}=\frac{\partial v}{\partial z}+\frac{\partial w}{\partial y};\ \gamma_{xz}=\frac{\partial u}{\partial z}+\frac{\partial w}{\partial x} \tag{2}$$

For laminated composite plates, the stress vector for the pth ply is

$$\{\sigma^{(p)}\}=[Q^{(p)}]\{\varepsilon\} \tag{3}$$

where $\{\sigma^{(p)}\}=\{\sigma_x, \sigma_y, \sigma_z, \tau_{xy}, \tau_{yz}, \tau_{xz}\}^{(p)T}$ and $[Q^{(p)}]$ is a matrix of stiffness coefficients for laminated orthotropicity.[7]

Eqs.(2) and (3) suggest that the strains and stresses are continuous, whereas some of the actual stress components $(\sigma_x, \sigma_y, \tau_{xy})$ are discontinuous across the infinitely thin bondlines between the ply layers.

Using Eqs.(1)~(3), the strain energy of the laminated composite plate (Fig. 1) is defined by the volume integral

$$U=\frac{1}{2}\iiint\{\sigma^{(p)}\}^T\{\varepsilon\}dV \tag{4}$$

where $dV=dxdydz$.

The total kinetic energy of the laminated plate is

$$T=\frac{1}{2}\iiint\rho^{(p)}(\dot{u}^2+\dot{v}^2+\dot{w}^2)dV \tag{5}$$

where $\rho^{(p)}$ is the mass density of the pth lamina of the plate and dots $(\cdot)$ indicate derivatives with respect to time.

For free vibrations, the displacement components of the laminated plate are assumed as simple harmonic, as follows,

$$u(x, y, z, t)=U_x(x, y, z)e^{j\omega t},$$
$$v(x, y, z, t)=V_y(x, y, z)e^{j\omega t},$$
$$w(x, y, z, t)=W_z(x, y, z)e^{j\omega t} \tag{6}$$

where ω is the circular frequency of vibration, e is the exponential function, t is time and $j=\sqrt{-1}$. The displacement amplitude functions are expressed in terms of algebraic polynomials, as follows:

$$U_x(x, y, z)=\sum_{l=1}^{L}\sum_{m=0}^{M}\sum_{n=0}^{N}A_{lmn}x^l y^m z^n,$$
$$V_y(x, y, z)=\sum_{l=1}^{L}\sum_{m=0}^{M}\sum_{n=0}^{N}B_{lmn}x^l y^m z^n,$$
$$W_z(x, y, z)=\sum_{l=1}^{L}\sum_{m=0}^{M}\sum_{n=0}^{N}C_{lmn}x^l y^m z^n \tag{7}$$

where z is measured from the mid-plane of the plate (see Fig. 1) and A_{lmn}, B_{lmn} and C_{lmn} are undetermined coefficients. Beginning the summation index $(l=1)$ in Eqs.(7) requires each terms of the series to satisfy the vanishing displacement conditions at the clamped edge of the plate (see Fig. 1), that is $U_x(0, y, z)=V_y(0, y, z)=W_z(0, y, z)=0$.

Substituting Eqs.(6) and (7) into (4) and (5) and setting the exponential terms unity, one obtains the maximum dynamic energies, which in turn are minimized with respect to the undetermined coefficients of the trial functions [Eqs.(7)]. Thus,

$$\frac{\partial}{\partial A_{lmn}}(U_{\max}-T_{\max})=0;\ \frac{\partial}{\partial B_{lmn}}(U_{\max}-T_{\max})=0;$$
$$\frac{\partial}{\partial C_{lmn}}(U_{\max}-T_{\max})=0 \tag{8}$$

where U_{max} is the maximum strain energy represented at the maximum displacement during a vibratory cycle, and T_{max} is the maximum kinetic energy represented at the maximum velocity during a vibratory cycle. The Ritz minimization indicated by Eqs.(8) results in $3\times L\times(M+1)\times(N+1)$ algebraic equations with undetermined coefficients (A_{lmn}, B_{lmn}, C_{lmn}). The vanishing determinant of these equations yields a set of eigenvalues(natural frequencies), with which a corresponding set of eigenvectors (mode shapes) may be computed.

3. Convergence Studies and Validation of 3-D Results

Using the 3-D Ritz procedure outlined in the previous section, it is now appropriate to address how many terms of the assumed displacement polynomials [Eqs.(7)] are required to yield reasonably accurate vibration solutions.

Table 1 summarizes a convergence study of the first six non-dimensional frequencies $\omega a^2\sqrt{\rho h/D_o}$ of four angle-ply square plates ($a/b=1$, $a/h=20$). In defining $\omega a^2\sqrt{\rho h/D_o}$, $D_o=E_{11}h^3/12(1-\nu_{12}\nu_{21})$ is the flexural rigidity apropos to plates having ply layers all oriented in the x-direction(i.e., the assumed stacking axis, $\theta=0°$). Hence, $\omega a^2\sqrt{\rho h/D_o}$ is invariant to the laminate stacking sequence and fiber orientation angle (θ). Numerical studies are performed for single-layer plates with unidirectional fiber orientation angle ($\theta=30°$), and for five-layer plates having stacking sequence (θ, $-\theta$, θ, $-\theta$, θ, with $\theta=30°$). Two types of fiber-reinforced epoxy materials are used in the convergence study, which are designated as[8] E-glass/epoxy (E/E) [$E_{11}=60.7$Gpa, $E_{22}=E_{33}=24.8$Gpa, $G_{12}=G_{13}=G_{23}=11.99$Gpa, $\nu_{12}=\nu_{13}=\nu_{23}=0.23$, $\rho=1.0$kg/m^3, $E_{11}/E_{22}=E_{11}/E_{33}=2.45$ (weak orthotropy)] and graphite/epoxy (G/E) [$E_{11}=138$Gpa, $E_{22}=E_{33}=8.98$Gpa, $G_{12}=G_{13}=G_{23}=7.1$Gpa, $\nu_{12}=\nu_{13}=\nu_{23}=0.30$, $\rho=1.0$kg/m^3, $E_{11}/E_{22}=E_{11}/E_{33}=$

Table 1 Convergence of frequency parameters $\omega a^2\sqrt{\rho h/D_o}$ of various cantilevered angle-ply plates ($a/b=1$, $a/h=20$)

Solution size	Mode number					
	1	2	3	4	5	6
(E/E$^+$) Single layer (30°)*						
6×6×4	2.949	7.051	17.84	19.74	25.73	40.90
7×7×4	2.945	7.045	17.77	19.60	25.65	40.26
8×8×4	2.944	7.022	17.76	19.59	25.60	40.09
(E/E) Five layer (30°, -30°, 30°, -30°, 30°)						
6×6×4	3.041	2.274	18.02	20.37	26.17	43.07
7×7×4	3.011	7.268	17.94	20.21	26.11	42.41
8×8×4	3.009	7.243	17.94	20.20	26.05	42.22
(G/E^{++}) Single layer (30°)						
6×6×4	2.077	4.502	9.799	12.87	17.87	20.37
7×7×4	2.071	4.494	9.688	12.80	17.73	20.07
8×8×4	2.067	4.484	9.683	12.76	17.62	19.89
(G/E) Five layer (30°, -30°, 30°, -30°, 30°)						
6×6×4	2.516	5.724	12.02	15.62	20.09	25.73
7×7×4	2.509	5.716	11.86	15.55	20.02	25.46
8×8×4	2.507	5.697	11.85	15.53	19.92	24.98

$^+$ E-glass/epoxy; $^{++}$ graphite/epoxy; * stacking sequence

15.4 (strong orthotropy)}.

Convergence of frequency results is shown in Table 1 as the solution size is increased from a 6×6×4 solution to a 8×8×4 solution. For instance, an 8×8×4 solution indicates that 8 terms in the x-direction, 8 terms in the y-direction, and 4-terms in the z-direction have been retained in the Ritz trial functions [Eqs.(7)] for a total of 3×(8×8×4)=768 degrees of freedom. Clearly, a reasonably good monotonic(three to four significant digit) convergence of frequencies for the first six modes is achieved using the present 3-D Ritz analysis. Indeed, the least upper bound frequency values obtained by using either a 7×7×4 or an 8×8×4 solution differ by less than one percent on the average.

The accuracy of the present 3-D analysis is partially validated by the frequency data shown in Table 2. Shown therein is a comparison of $\omega a^2\sqrt{\rho h/D_o}$ for isotropic and symmetrically-laminated composite square plates ($a/b=1$, $a/h=20$). Material properties of the Hercules AS1/3501-6 graphite/epoxy plates examined in Table 2 are as follows[1] : $E_{11}=128$Gpa, $E_{22}=E_{33}=11$Gpa, $G_{12}=G_{13}=4.48$Gpa, $G_{23}=1.53$Gpa, $\nu_{12}=\nu_{13}=\nu_{23}=0.25$, $\rho=1.5\times10^3$kg/m^3, $t_p=0.13$mm, $E_{11}/E_{22}=E_{11}/E_{33}=11.56$ (strong orthotropy).

As can be seen in Table 2, the appreciable effects of transverse shear and normal strains and rotary inertia exhibited by the 3-D solutions yield lower upper bounds on the true $\omega a^2\sqrt{\rho h/D_o}$ values compared to those values obtained from alternative mathematical models, which are the superposition method for an isotropic Kirchhoff-Love thin plate ($\nu=0.333$)[9], and the finite element method[1] and Ritz method[5] in conjunction with CLT for the angle-ply plates. The 3-D results obtained using an 8×8×4 solution yields a variation in z for the transverse normal and shear strains, which approximate the actual non-uniform strain variation through the thickness of the laminae. Comparing the isotropic and Hercules graphite/epoxy plate frequency data in Table 2, it is shown that the frequency decreasing effect of shear deformation and rotary inertia is most significant in the higher modes of symmetrically-laminated composite plates with a large number of ply layers at high fiber

Table 2 Comparison of frequency parameters $\omega a^2\sqrt{\rho h/D_o}$ of cantilevered plates ($a/b=1$, $a/h=20$)

Source	Mode number				
	1	2	3	4	5
Isotropic ($\nu=0.333$)					
[1]Present 3-D	3.470	8.239	20.89	26.61	29.83
[2]Narita & Leissa[5]	3.459	8.358	21.09	27.07	30.56
[3]Gorman[8]	3.459	8.356	21.09	27.06	30.55
(G/E) Four layer (0°, 30°, 30°, 0°)					
[1]Present 3-D	3.354	4.564	9.482	19.35	19.77
[2]Narita & Leissa[5]	3.409	4.725	9.874	20.78	23.32
[4]Crawley[1]	3.379	4.468	9.827	21.44	22.05
[5]Crawley[1]	3.021	4.670	9.395	18.69	19.39
(G/E) Eight layer (45°, -45°, -45°, 45°, 45°, -45°, -45°, 45°)					
[1]Present 3-D	1.754	6.112	9.765	15.92	19.20
[2]Narita & Leissa[5]	1.813	6.553	10.48	17.29	21.49
[4]Crawley[1]	1.792	6.443	10.38	17.11	21.26
[5]Crawley[1]	1.692	6.089	10.20	15.07	19.17

[1] 8×8×4 solution; [2] Ritz method using CLT; [3] finite element method using CLT; [4] finite element method using 8-noded moderately thick shallow shell element; [5] experiment test results

orientation angles. It appears that experimental data reported by Crawley[1] are lower than the analytical results. This may be due to the difficulty in obtaining rigid clamping in the experiments.

In Tables 3 and 4, the first six frequency parameters $\omega a^2\sqrt{\rho h/D_o}$ of the E/E and G/E plates obtained using the present 3-D method are compared with upper bound $\omega a^2\sqrt{\rho h/D_o}$ values reported recently by Narita and Leissa.[5] Results are shown for single-layer (θ) and five-layer ($\theta, -\theta, \theta, -\theta, \theta$) square plates ($a/b$=1, a/h=20) and fiber angle θ varying from 0° to 90°.

Among the significant frequency trends in Tables 3 and 4, one can cite the following which are common to those derived from the present 3-D Ritz analysis and the CLT Ritz procedure by Narita and Leissa.[5] First of all, the

Table 3 Effects of varying θ upon the frequency parameters $\omega a^2\sqrt{\rho h/D_o}$ of cantilevered E-glass/epoxy (E/E) plates (a/b=1, a/h=20)

θ (degrees)	Mode number					
	1	2	3	4	5	6
Single layer (θ)						
0	3.497[+] (3.507)[++]	6.775 (6.897)	18.04 (18.41)	21.58 (22.07)	26.52 (27.37)	40.35 (42.14)
15	3.320 (3.331)	6.875 (7.005)	18.23 (18.61)	20.70 (21.16)	26.20 (27.06)	40.15 (41.74)
30	2.944 (2.954)	7.022 (7.164)	17.76 (18.14)	15.59 (20.01)	25.60 (26.45)	40.09 (41.68)
45	2.591 (2.598)	6.965 (7.110)	15.86 (16.13)	19.98 (20.42)	25.13 (25.96)	40.06 (41.66)
60	2.363 (2.366)	6.613 (6.742)	14.53 (14.71)	20.57 (21.01)	24.80 (25.52)	39.73 (41.20)
75	2.262 (2.263)	6.189 (6.296)	13.97 (14.12)	20.96 (21.45)	24.52 (25.07)	38.64 (39.69)
90	2.238 (2.239)	6.006 (6.104)	13.86 (13.99)	21.03 (21.56)	24.46 (24.91)	38.27 (39.27)
Five layer ($\theta, -\theta, \theta, -\theta, \theta$)						
0	3.497 (3.507)	6.775 (6.897)	18.04 (18.41)	21.58 (22.07)	26.52 (27.37)	40.35 (42.14)
15	3.354 (3.364)	6.957 (7.091)	18.32 (18.72)	20.88 (21.33)	26.42 (27.29)	40.98 (42.67)
30	3.009 (3.019)	7.243 (7.399)	17.94 (18.32)	20.20 (20.65)	26.05 (26.95)	42.22 (44.05)
45	2.635 (2.643)	7.245 (7.408)	16.01 (16.27)	21.04 (21.55)	25.31 (26.18)	42.82 (44.79)
60	2.376 (2.380)	6.847 (6.989)	14.57 (14.75)	21.86 (22.38)	24.38 (25.10)	40.57 (41.83)
75	2.263 (2.265)	6.282 (6.394)	13.98 (14.12)	21.53 (22.08)	24.26 (24.76)	38.69 (39.73)
90	2.238 (2.239)	6.006 (6.104)	13.86 (13.99)	21.03 (21.56)	24.46 (24.91)	38.27 (39.27)

[+] Present 3-D(8×8×4 solution); [++] Results in parentheses cf. Narita & Leissa[5](CPT)

Table 4 Effects of varying θ upon the frequency parameters $\omega a^2\sqrt{\rho h/D_o}$ of cantilevered graphite/epoxy (G/E) plates ($a/b=1$, $a/h=20$)

θ (degrees)	Mode number					
	1	2	3	4	5	6
Single layer(θ)						
0	3.474' (3.514)''	4.631 (4.740)	8.846 (9.116)	17.77 (18.35)	20.43 (22.02)	21.84 (23.61)
15	2.899 (2.940)	4.632 (4.748)	9.225 (9.531)	17.33 (18.33)	18.28 (19.35)	20.87 (22.42)
30	2.067 (2.098)	4.484 (4.606)	9.683 (10.00)	12.76 (13.57)	17.62 (18.53)	19.89 (20.96)
45	1.466 (1.482)	4.098 (4.221)	9.082 (9.422)	10.14 (10.45)	16.45 (17.23)	19.70 (20.60)
60	1.105 (1.112)	3.553 (3.646)	6.912 (7.034)	10.21 (10.48)	16.62 (17.21)	19.52 (20.30)
75	0.936 (0.937)	3.106 (3.164)	5.839 (5.884)	10.04 (10.29)	16.13 (16.45)	19.17 (19.77)
90	0.896 (0.894)	2.933 (2.978)	5.572 (5.604)	9.861 (10.10)	15.43 (15.69)	19.97 (20.63)
Five layer (θ, −θ, θ, −θ, θ)						
0	3.474 (3.514)	4.631 (4.740)	8.846 (9.116)	17.77 (18.35)	20.43 (22.02)	21.84 (23.61)
15	3.160 (3.199)	5.072 (5.233)	10.02 (10.45)	18.79 (19.97)	19.21 (20.38)	21.85 (23.50)
30	2.507 (2.546)	5.697 (5.952)	11.85 (12.63)	15.53 (16.43)	19.92 (21.55)	24.98 (26.72)
45	1.770 (1.803)	5.706 (5.988)	10.23 (10.72)	14.98 (15.83)	19.01 (20.46)	29.98 (32.62)
60	1.210 (1.222)	4.917 (5.121)	7.331 (7.490)	14.77 (15.54)	18.10 (18.94)	22.55 (23.65)
75	0.949 (0.949)	3.671 (3.765)	5.887 (5.933)	11.80 (12.21)	16.29 (16.62)	21.20 (22.00)
90	0.896 (0.894)	2.933 (2.978)	5.572 (5.604)	9.861 (10.10)	15.43 (15.69)	19.97 (20.63)

' Present 3-D (8×8×4 solution); '' Results in parentheses cf. Narita & Leissa[5](CPT)

fundamental frequency of the plate laminates strictly decreased as the fiber angle (θ) is increased with in the range $0°\leq\theta\leq90°$. The decreasing trend with increasing θ is more pronounced for the G/E plates than the E/E ones, since the G/E plates have greater longitudinal rigidity associated with spanwise bending of the lowest frequency mode. In the higher mode 2-6, however, the variation of $\omega a^2\sqrt{\rho h/D_o}$ exhibits an increase before a gradual decrease or vice-versa as θ increases. The latter is an interesting trend which is more pronounced in the higher modes of the five-layer, alternating angle-ply plate than the single-layer plate having parallel fibers.

Attention is now given to a comparison of the 3-D and CLT $\omega a^2\sqrt{\rho h/D_o}$ values in Tables 5 and 6 for cross-ply E/E and G/E laminated

Table 5 Frequency parameters $\omega a^2\sqrt{\rho h/D_o}$ of cantilevered E-glass/epoxy(E/E) plates (a/h=20)

a/b	NP^*	Mode number					
		1	2	3	4	5	6
0.5	1	3.502[+] (3.511)[++]	4.606 (4.646)	7.690 (7.787)	13.33 (13.52)	21.45 (21.85)	22.88 (22.65)
	3	3.464 (3.473)	4.579 (4.618)	7.717 (7.812)	13.51 (13.70)	21.25 (21.68)	22.67 (23.00)
	5	3.282 (3.288)	4.449 (4.486)	7.832 (7.924)	14.28 (14.47)	20.20 (20.58)	21.69 (22.18)
1	1	3.497 (3.507)	6.775 (6.897)	18.04 (18.41)	21.58 (22.07)	26.52 (27.37)	40.35 (42.14)
	3	3.459 (3.468)	6.753 (6.874)	18.31 (18.67)	21.37 (21.84)	26.36 (27.19)	40.37 (42.15)
	5	3.277 (3.284)	6.646 (6.764)	19.29 (19.65)	20.54 (20.94)	25.55 (26.32)	40.45 (42.17)
2	1	3.499 (3.499)	11.42 (11.58)	21.78 (21.90)	38.58 (39.19)	59.15 (59.86)	61.83 (62.60)
	3	3.461 (3.461)	11.40 (11.56)	21.55 (21.66)	38.44 (39.05)	59.28 (60.02)	62.45 (63.18)
	5	3.279 (3.279)	11.28 (11.44)	20.43 (20.52)	37.79 (38.37)	56.76 (57.40)	67.91 (68.71)

* Number of plies: N=1(0°); N=3(0°, 90°, 0°); N=5(0°, 90°, 0°, 90°, 0°)
[+] Present 3-D (8×8×4 solution); [++] Results in parentheses cf. Narita & Leissa[5](CPT)

Table 6 Frequency parameters $\omega a^2\sqrt{\rho h/D_o}$ of cantilevered graphite/epoxy(G/E) plates (a/h=20)

a/b	NP^*	Mode number					
		1	2	3	4	5	6
0.5	1	3.476[+] (3.515)[++]	3.796 (3.850)	4.849 (4.946)	6.892 (7.051)	10.75 (10.42)	16.35 (15.19)
	3	3.417 (3.454)	3.749 (3.801)	4.933 (5.029)	7.436 (7.595)	12.20 (11.83)	19.18 (17.82)
	5	3.128 (3.155)	3.503 (3.546)	5.254 (5.341)	9.494 (9.680)	17.19 (16.85)	18.66 (19.77)
1	1	3.474 (3.514)	4.631 (4.740)	8.846 (9.116)	17.77 (18.35)	20.43 (22.02)	21.84 (23.61)
	3	3.416 (3.453)	4.598 (4.707)	9.738 (10.01)	20.14 (21.57)	20.79 (21.64)	21.73 (23.33)
	5	3.128 (3.155)	4.404 (4.505)	13.02 (13.33)	18.65 (19.77)	20.24 (21.55)	26.86 (28.80)
2	1	3.503 (3.513)	6.957 (7.068)	21.54 (21.97)	25.51 (25.84)	27.14 (27.84)	45.11 (46.60)
	3	3.443 (3.452)	6.929 (7.040)	21.22 (21.62)	26.92 (27.60)	30.33 (30.70)	47.89 (49.40)
	5	3.148 (3.155)	6.754 (6.862)	19.47 (19.76)	25.66 (26.26)	46.32 (47.09)	53.44 (53.35)

* Number of plies: N=1(0°); N=3(0°, 90°, 0°); N=5(0°, 90°, 0°, 90°, 0°)
[+] Present 3-D (8×8×4 solution); [++] Results in parentheses cf. Narita & Leissa[5](CPT)

plates. Frequency results are shown for single-layer [0°], three-layer [0°, 90°, 0°] and five layer [0°, 90°, 0°, 90°, 0°] plates(with layers sequences shown in brackets). Although not shown, the mode shapes for these cross-ply plates may be classified as either symmetric or antisymmetric, depending on the layer sequences. The influence of the number of ply (NP) on $\omega a^2\sqrt{\rho h/D_o}$ is explicitly understood in Tables 5 and 6, since the frequency data is normalized with respect to the plate thickness h. The first and second frequencies are observed to decrease with increasing NP, whereas the higher frequencies do not exhibit specific monotonic trends.

4. Concluding Remarks

The first known 3-D continuum vibration solutions for laminated composite cantilevered plates have been reported in this work. The Ritz method has been employed to determine approximate non-dimensional frequencies. The dynamical energies of the laminated plate have been derived from a 3-D elasticity-based, structural body comprising of a number of orthotropic parallelepiped layers with thickness t_p, fiber orientation angle θ. A set of algebraic polynomials, which is mathematically complete, has been utilized as displacement trial functions. No additional kinematics constraints (as in conventional plate theories) have been imposed in constructing the dynamical energies of the plate laminates, except the vanishing displacements at the clamped edge, thereby guaranteeing monotonic convergence from above to the exact frequencies, as sufficient number of polynomial terms are used.

Given that the effects of transverse shear and normal strains, rotary inertia, and other complicated kinematics are inherent in the current 3-D lamination model, an improvement of the existing vibration database of the subject problem generated from classical lamination theory is evident by the presented results. Hence, the present 3-D approach provides an efficient model of forecasting shear deformable vibration characteristics of thin and thick, laminated composite plates. The significance of this work provides structural dynamists with an accurate 3-D model that permits efficient theoretical experimentation of laminated composite plate dynamics over a wide range of geometrical and material property parameters.

References

1. Crawley, E. F., "The natural modes of graphite/epoxy cantilever plates and shells," *Journal of Composite Materials*, Vol. 13, 1979, pp.195~205
2. Crawley, E. F. and Dugundji, J., "Frequency determination and non-dimensionalization for composite cantilever plates," *Journal of Sound and Vibration*, Vol. 72, 1980, pp.1~10
3. Jensen, D. W. and Crawley, E. F., "Frequency determination technique for cantilevered plates with bending-torsion coupling," *AIAA Journal*, Vol. 22, 1984, pp.415~420
4. Baharloy, B. and Leissa, A. W., "Vibration and buckling of generally laminated composite plates with arbitrary edge conditions," *International Journal of Mechanical Sciences*, Vol. 29, No. 8, 1987, pp.545~555
5. Narita, Y. and Leissa, A. W., "Frequencies and mode shapes of cantilevered laminated composite plates," *Journal of Sound and Vibration*, Vol. 154, No. 1, 1992, pp.161~172
6. Leissa, A. W., "Advances in vibration, buckling and postbuckling studies on composite plates," In *Composite Structures*, Ed. By I. H. Marshall, Elsevier Applied Science Publishers, London, 1981
7. Jones, R. M., *Mechanics of Composite Materials*,

Scripta, Washington, D.C., 1975
8. Vinson, J. R. and Sierakowski, R. L., *The Behavior of Structures Composed of Composite Materials*, Dordrecht: Martinus Nijhoff, 1986.
9. Gorman, D. J., "Free vibration analysis of cantilever plates by the method of superposition," *Journal of Sound and Vibration*, Vol. 49, 1976, pp.453~467